Available online at www.sciencedirect.com

ScienceDirect

journal homepage: www.elsevier.com/locate/issn/15375110

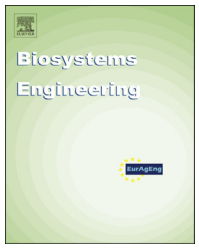

Special Issue: Irrigated Agriculture

Research Paper

Prototype emitter for use in subsurface drip irrigation: Manufacturing, hydraulic evaluation and experimental analyses

Wanderley de Jesus Souza [a,*], *Leonor Rodrigues Sinobas* [b], *Raúl Sánchez* [b], *Tarlei Arriel Botrel* [c], *Rubens Duarte Coelho* [c]

[a] *Federal University of the West of Bahia, Center of Sciences and Technologies, 47808021, Barreiras, Bahia, Brazil*
[b] *Polytechnic University of Madrid, Research Group Hydraulic for Irrigation, 28040, Madrid, Spain*
[c] *University of São Paulo, Department of Biosystems Engineering, 13418-900, Piracicaba, São Paulo, Brazil*

ARTICLE INFO

Article history:
Published online 3 October 2014

keywords:
Subsurface drip irrigation
Emitter design
Root intrusion

The current research aims to analyse theoretically and evaluate a self-manufactured simple design for subsurface drip irrigation (SDI) emitter to avoid root and soil intrusion. It was composed of three concentric cylindrical elements: an elastic silicone membrane; a polyethylene tube with two holes drilled on its wall for water discharge; and a vinyl polychloride protector system to wrap the other elements. The discharge of the emitter depends on the change in the membrane diameter when it is deformed by the water pressure. The study of the operation of this emitter is a new approach that considers mechanical and hydraulic principles. Thus, the estimation on the membrane deformation was based on classical mechanical stress theories in composite cylinders. The hydraulic principles considered the solid deformation due to force based on water pressure and the general Darcy–Weisbach head-loss equation. Twenty emitter units, with the selected design, were handcrafted in a lathe and were used in this study. The measured pressure/discharge relationship for the emitters showed good agreement with that calculated by the theoretical approach. The variation coefficient of the handcrafted emitters was high compared to commercial emitters. Results from field evaluations showed variable values for the relative flow variation, water emission uniformity and relative flow rate coefficients, but no emitter was obstructed. Therefore, the current emitter design could be suitable for SDI following further studies to develop a final prototype.

* *Corresponding author*. Tel.: +55 77 36143100; fax: +55 77 3614 3514.
E-mail addresses: wanderley.souza@ufob.edu.br, wjsouzaufba@gmail.com, wanderley.souza@ufba.br (W.J. Souza), leonor.rodrigues.sinobas@upm.es (L.R. Sinobas), raul.sanches@upm.es (R. Sánchez), tabotrel@usp.br (T.A. Botrel), rdcoelho@usp.br (R.D. Coelho).
http://dx.doi.org/10.1016/j.biosystemseng.2014.09.011
1537-5110/

Nomenclature

B	contraction value, mm
CAD	computer-aided design
CUE	water emission uniformity coefficient, %
CV_m	variation coefficient of manufacture, %
CV_{QR}	variation coefficient of relative flow, %
d	Willmott's concordance index
d_c	equivalent membrane diameter after contraction, mm
d_h	contact diameter, mm
d_i	inside membrane diameter, mm
d_o	outside envelope protector diameter, mm
DQ	disturbance of emitter flow, %
d_s	external pipe diameter, mm
E	elasticity module, kPa
E_i	estimated flow data, l h^{-1}
$\overline{E}$	average estimated flow data, l h^{-1}
f	friction factor
g	gravity acceleration, m s^{-2}
H	head loss, m
L	membrane length, m
n	number of data
O_i	observed data, l h^{-1}
$\overline{O}$	mean observed flow data, l h^{-1}
p_c	contact pressure, kPa
PE	polyethylene
p_i	internal pressures, kPa
p_s	external pressure, kPa
PVC	vinyl polychloride
q	emitter flow, l h^{-1}
q_m	average emitter discharge, l h^{-1}
q_{min}	minimum emitter discharge, l h^{-1}
QR	relative flow rate
Q_1	average flow rate at the start tests, l h^{-1}
Q_2	average flow rate at the end tests, l h^{-1}
r	Pearson's correlation coefficient
R_H	hydraulic radius, m
r_i	inside membrane radius, mm
SDI	subsurface drip irrigation
SS	bare soil
SC	sugar cane
Δd_h	changes in the contact diameter, mm
Δd_i	changes inside the membrane diameter, mm
Δd_s	changes in the external pipe diameter, mm
ΔL	length variation, m
Δv_i	velocity of water, m s^{-1}
V	Poisson coefficient
σ	emitter's discharge standard deviation, l h^{-1}
σ_{QR}	standard deviation of relative flow rate, l h^{-1}
σ_t	tangential tension, N m^{-2}

1. Introduction

Subsurface Drip Irrigation (SDI) is similar to surface drip irrigation but the emitters are located below the soil surface and thus the water is applied directly into the root zone. It has been used for the last 40 years and is suitable for most crops, particularly for high value fruit and vegetable as well as for turf and landscapes. A drawback is that its irrigation uniformity can be severely affected by the obstruction of an emitter, although some field evaluations have shown uniformity coefficients similar to or even higher than those from drip irrigation (Rodríguez-Sinobas, Gil, Sánchez, & Benitez, 2012).

The emitter is a key component to obtain high irrigation uniformity. However in SDI, obstructions caused by soil particle suction and root intrusion can occur more quickly than for surface emitters, and this is a major current concern. Emitter obstruction due to chemical, physical or biological causes has been extensively investigated and documented. Chemical obstruction, mainly resulting from the presence of carbonates within the irrigation water, is preventable if acid injections are added to it. Root penetration through emitters can be characterised as a biological and physical obstruction mechanism, although some procedures can minimise and/or avoid such intrusion: water management, chemical treatment and emitter design with physical devices have been suggested (Cloi & Suarez-Rey, 2004; Coelho, Faria, & Mélo, 2006).

The main treatments to avoid root intrusion require the application of a dilute acid or a herbicide. Trifuralin is the usual herbicide used because it is strongly adsorbed by the soil colloids and limits root growth in the emitter's neighbourhood (Dasberg & Or, 1999). However, this herbicide has been banned since 2008 in countries in the European Union (Regulation – EC 1107/2009). Chlorine and acid applications may also be used as a preventive action but it is a costly one since they require frequent maintenance and may harm the environment. According to the University of California (2008, 19 pp), acid application with irrigation water at pH < 4.0 may damage the emitters. The injection of Trifluralin into the irrigation water or its incorporation to filters and emitters has been suggested as a potential alternative, although such practice is not always economically feasible (Suarez-Rey, Choi, McCloskey, & Kopec, 2006). Moreover, the use of chemicals can be harmful to the environment.

Designing emitter prototypes capable of avoiding suction of soil particles and root intrusion might prevent emitter obstructions and make such emitters a feasible technical, economic and environmental alternative. There are several studies in the literature that have addressed emitter obstruction for drip irrigation. Abdulqader and Mohammed (2013) developed a surface drip irrigation emitter using a 3D Computer-Aided Design (CAD) which showed a better anti-obstruction performance than that of previous designs when tested under laboratory conditions. Hernandez (2010) tested an emitter protection system composed of a plastic soda bottle and rice husks for use to subsurface drip irrigate a fig crop. There was no root intrusion when the emitter was protected by the plastic soda bottle system. However, the rice husks proved not to be as efficient during the nine month study. As the tested systems were handmade, their large scale production may be difficult and, in addition, their performance would need to be tested over a long period in crops with roots more aggressive than those of figs. Mosca,

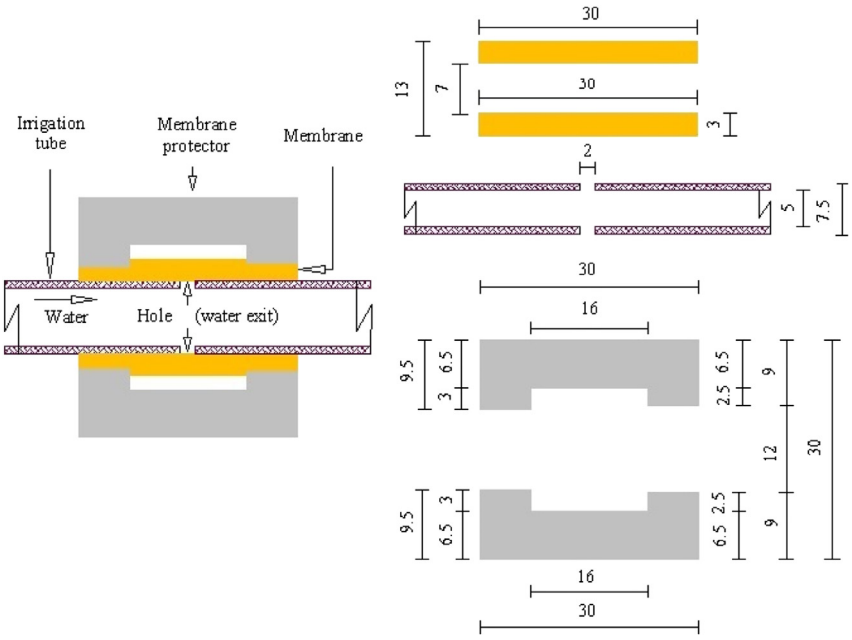

Fig. 1 – Scheme showing the elements of the emitter (length units are expressed in mm).

Testezlaf, and Gomes (2005) developed an emitter model for low pressure SDI by making holes in a polyethylene tube and crossing strings across the orifices. This system led to lower emitter flow rates. Its performance was assessed by observing water distribution in a bare soil under laboratory conditions. The authors highlighted the system's potential to save water although it requires further evaluation under field crop conditions.

Most emitter designs do not consider the hydraulic-mechanical operation to avoid emitter obstruction, although it might have some potential to do so. Hence, the current study aims at manufacturing (on a small scale) and testing an SDI emitter based on a mechanical-hydraulic operation capable of reducing or preventing the intrusion of root and soil particles without the need for chemical applications. On one hand, this particular design could combine effects from the operation of hydraulic elements with the opening and shutting down of irrigation valves; and, on the other hand, the discharge of the emitter could be regulated by the deformation of an elastic membrane (mechanical element). The current study also presents a new approach which considers the basic principles of fluid mechanics and material deformation under stress for the estimation of pressure and discharge in the emitter. Finally, the performance of the emitter was assessed under laboratory and field conditions.

2. Material and methods

The activities performed to achieve the aims of the current study were divided into three stages: to show the emitter design described in Section 2.1; to model the hydraulic and mechanical principles described in Section 2.2 and to set up the experimental frame described in Section 2.3.

2.1. *Emitter design*

Most commercial emitter designs lose pressure through their labyrinthine geometry which requires specific tools for manufacture. Computational fluid dynamic technology is also used for assessing pressure losses. However, the present study intended to follow a different approach: to develop an emitter design in which operation could be explained by hydraulic and mechanical principles. Its geometry should be easily handcrafted and its raw materials should be available in the market. Moreover, it should be able to avoid obstructions by root and soil intrusion at the emitter's outlet, without the use of chemical products. Based on these requirements, approximately 30 different emitter design geometries were considered (some of them were also handcrafted) before selecting the design presented herein.

The chosen emitter design was composed of three cylindrical elements: a polyethylene pipe (irrigation tube) with two holes drilled in its walls to allow water discharge; an elastic silicon membrane as the mechanical element in the system; and a vinyl polychloride PVC protection tube surrounding the other two elements. These materials were available in the market as well as being easily handcrafted. Likewise, the PVC and polyethylene materials are frequently used in drip irrigation.

On the one hand, the elastic membranes are typical elements for compensating emitters to keep a constant discharge within an operation interval. These elements modify their shape under pressure; they vary the surface flow path and keep the discharge constant. However, their mechanical behaviour has not yet been reported in the literature and neither has their use in non-compensating emitters been reported. On the other hand, emitter manufacturers are seeking new emitter designs able to reduce production costs. Therefore, the cylindrical geometry is

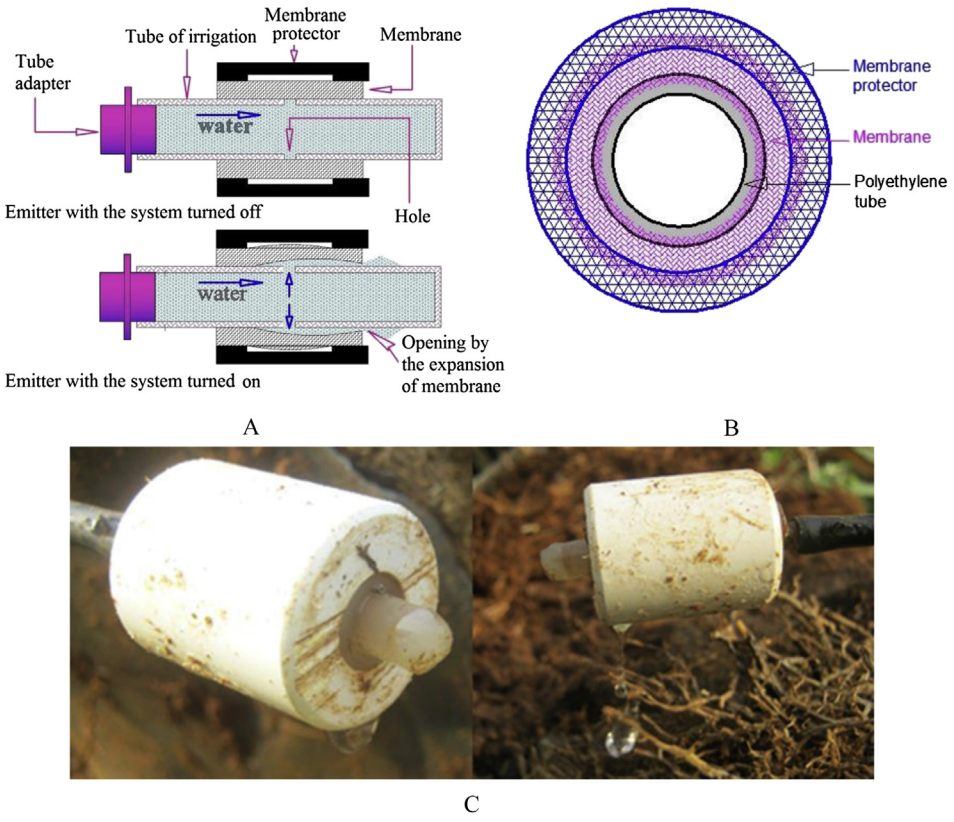

Fig. 2 – Sketch of the emitter's operation process (A) and detail of the assembly among the three emitter's elements: polyethylene tube, membrane and membrane protector (B, C).

simpler than a labyrinthine one and it may reduce the cost of emitters.

The prototype of the selected emitter design was handcrafted on a lathe. Figure 1 shows a scheme with the emitter elements and their dimensions. The polyethylene tube had an inner diameter of 5.0 mm and outer diameter of 7.5 mm. The water was discharged through two holes of 2.0 mm each. The membrane was 30.0 mm long with inside and outside diameters of 7.0 and 13.0 mm, respectively. The protector tube was 30.0 mm long with internal and external diameter of 12.0 and 30.0 mm, respectively. The tube was cut and carefully drilled during membrane insertion on both sides of the wrapping tube. The right hand side had a reduction of 2.5 mm and the left hand side of 3.0 mm (see Fig. 1).

It is worth noting that the inner diameter of the membrane was smaller than the outer diameter of the tube. The outer diameter of the membrane was bigger than the inner diameter of the envelope. These detailed measures ensure proper contact pressure between all the elements of the emitter (tube, membrane and envelope). Thus, they minimise the risk of intrusion by root and soil particles.

The size of the emitter was based on the size of those that have been commercialised and it was also adequate to test the emitter in laboratory equipment. Nevertheless, further studies on other sizes for commercial application must be performed if the prototype design proves acceptable for commercial use. The current paper is focused on the emitter's operation principles, as a precursor to any commercial development. If there is a change in the emitter's scale, a dimensional and similarity analysis should be done in order to study its performance at the new scale.

Although the production process was simple, only 24 units were handcrafted since the aim was to assess the performance of the design rather than attempt large scale manufacture of emitters, which would also require specific equipment. Though care was taken during emitter manufacturing, but it was impossible to get two emitter units with exactly the same lengths, and this had an impact on the emitter's coefficient of variation.

The emitter discharge depends on variations in the diameter of the membrane which deforms under water pressure. When irrigation starts, the membrane diameter is expanded (see Fig. 2A). The greater the change, the higher is the flow rate in the emitter. When irrigation stops, the pressure drops down to zero and the membrane goes back to its initial condition (see Fig. 2A). Figure 2 (B) shows a sketch of a transverse section with the emitter elements and Fig. 2 (C) shows two views of the emitters. According to the presented emitter model, the membrane is always compressed between the tube and the protector. However, such compression gets stronger when the irrigation system is turned on and it gets less when the system is off (see Fig. 2A). If the membrane's material has poor elasticity, it may get thinner and allow the water to exit but, if the material's elasticity is good, the membrane should be compressed and expanded as the system is turned off and on, respectively, thus avoiding the incursion of roots inside the emitter.

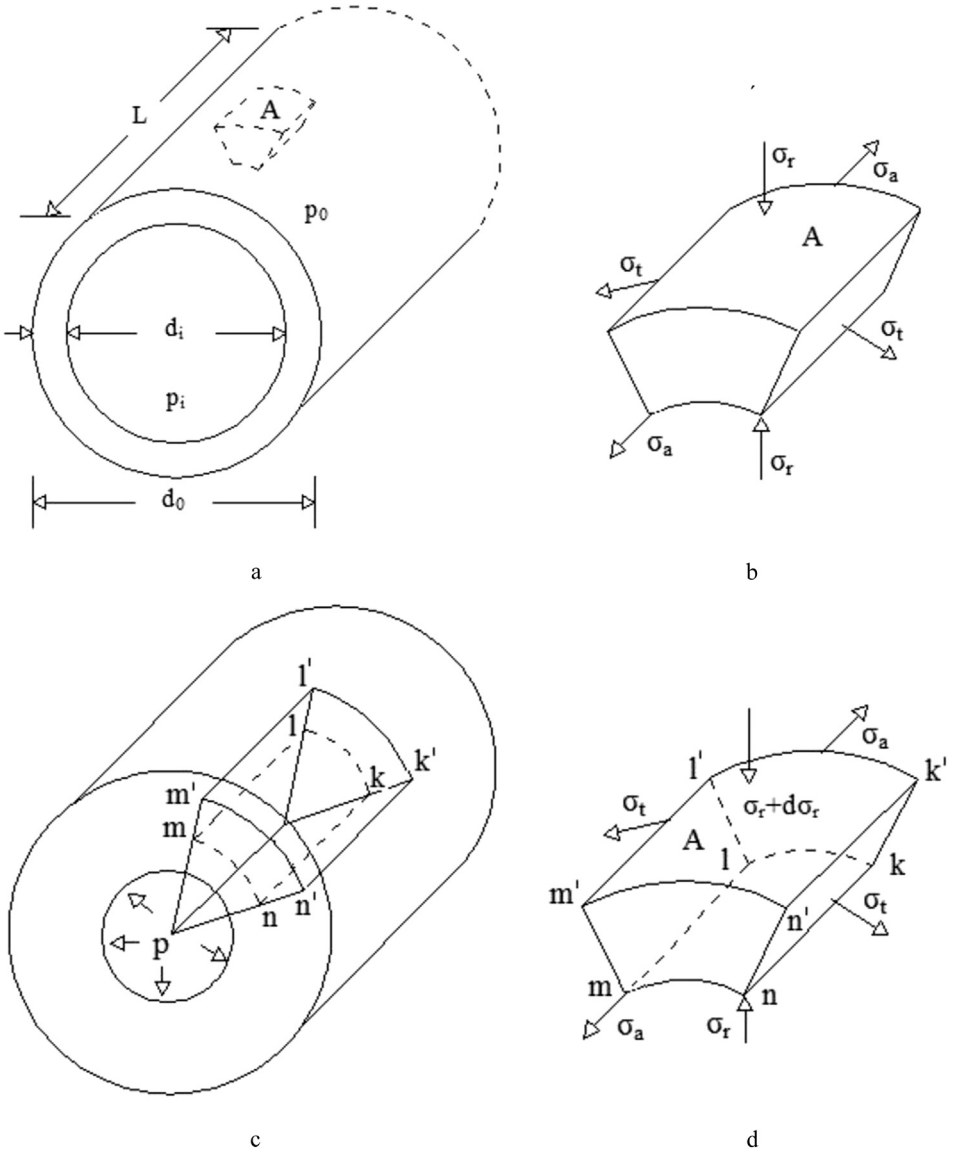

Fig. 3 – Thin-wall membrane (a), stress on the thin-wall membrane element (b), thick-wall membrane (c), and stress on the thick-wall membrane element (d).

2.2. *Modelling the hydraulic and mechanical principles*

The general deformation theories are suitable to study the material mechanics as well as being applied in the irrigation engineering field. Thus, they can be used to explain the behaviour of an emitter composed of a cylindrical membrane and a protector tube. A sketch of the thin-walled membrane (length L, inward diameter d_i, and outward diameter d_0 and thickness t) is depicted in Fig. 3a, and the one for the thick-walled membrane is shown in Fig. 3c. The membrane walls are stressed under the internal pressure p_i, or external p_0 but thick-walled membranes can support both pressures at the same time. The stress can be characterised by three components (see Fig. 3b and d): axial tension (σ_a), tangential tension (σ_t) and radial tension (σ_r). The last component is considered negligible in thin-walled membranes.

The emitter prototype in this paper contains a thick-walled membrane, the emitter element, that mainly suffers deformation to enable water discharge and avoid emitter obstruction by the membrane contraction. It is therefore important to study the diameter variations in the membrane. In order to do so, σ_a, σ_t and σ_r have to be analysed at every point along the membrane following the Lamé problem (Hearn, 1997).

The scheme of a membrane (inside diameter d_i, outside diameter d_0, thickness t and length L) under an internal pressure p_i and external pressure p_0 is shown in Fig. 4. This illustrates the tensions and deformations produced within a transversal membrane section (inner radius r and thickness d_r). Tension σ_a is considered uniform along the thickness. If the Poisson coefficient (ν), characterising the transversal deformation, and the material elasticity module (E), characterising the traction and contraction of materials, are known, the tension components can be obtained as a function of the variables mentioned above, as will be described by Eqs. (1)–(5).

These theories can explain the membrane diameter variation when subjected to the variation of water pressure in the

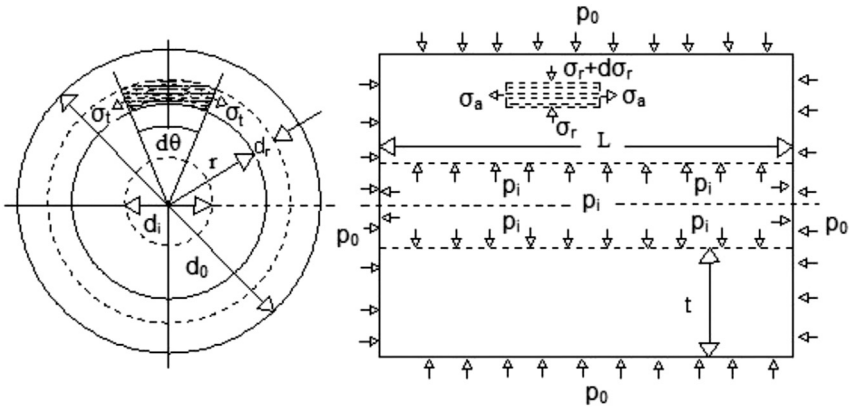

Fig. 4 – Illustrative scheme showing the parameters: d_i, d_0, t, L, p_i and p_0 for calculations of stresses and deformations in the membrane.

emitter, by considering the Lamé Equations applied to the membrane. Thus, Equations (1)–(5) were developed applying the equations of Lamé, Clavarino and Birnie as described by Hearn (1997). The Lamé equation was used to study the behaviour of a membrane subjected to stress; the Clavarino equation was used for analysing a closed membrane and the Birnie equation for an opened one. Details regarding the development of these equations have been given by de Jesus Souza (2010), Section 4.1.3.

The elastic membrane diameter varies with the emitter pressure and this will affect emitter discharge. Even if the variation in the emitter were small, it can still make a significant change for the emitter discharge. Figure 5 completes the information given in Figs. 3(d) and 4, showing the tangential tensions within the membrane caused by the water pressure and by the insertion of the polyethylene tube into the membrane. There is a mass element which handles a unitary tangential stress σ_t within the elastic membrane exposed to the emitter pressure which comes from a certain point in the centre of the membrane.

The radial stress on the contact surfaces between the polyethylene tube and the membrane depends on the Poisson coefficient (ν), the elasticity module (E) and on the difference between the membrane inner diameter and the polyethylene tube outer diameter. Thus, the unitary variation of the membrane inner diameter (Δd_i), subject to internal pressures (p_i), is described according to the Hook's Law:

$$\Delta d_i = \frac{p_i \cdot d_i}{E}\left[\frac{\left(d_S{}^2 + d_i{}^2\right)}{\left(d_S{}^2 - d_i{}^2\right)} + \nu\right] \quad (1)$$

If the membrane only experiences the external pressure (p_s), its outer diameter reduces, thus resulting in:

$$\Delta d_S = \frac{p_S \cdot d_S}{E}\left[\frac{\left(d_S{}^2 + d_i{}^2\right)}{\left(d_S{}^2 - d_i{}^2\right)} - \nu\right] \quad (2)$$

where d_s stands for the diameter variation maximum value.

According to Fig. 5, the diameter deformation by stress on the contact surface may be calculated by:

$$\begin{aligned} \Delta d_s &= d_s - d_c \\ \Delta d_h &= d_c - d_h \\ \Delta d_s + \Delta d_h &= d_s - d_h \therefore B = d_s - d_h \end{aligned} \quad (3)$$

where B is the contraction value corresponded to the membrane deformation by stress on the contact surface.

B is not a numerical value aiming to show that the water leaks into the soil but it is a combined result caused by the pressure operation. Such operation compresses the membrane and reduces membrane wall thickness by membrane insertion into both the protector and the polyethylene tube, since the membrane presents a smaller inner diameter than that presented by the tube outer diameter and the outer diameter is bigger than the protector's inner diameter. The contraction value may be obtained from laboratory tests or may come from knowledge of the elasticity module, the Poisson coefficient, the operation pressure and the inner diameters of the emitter elements.

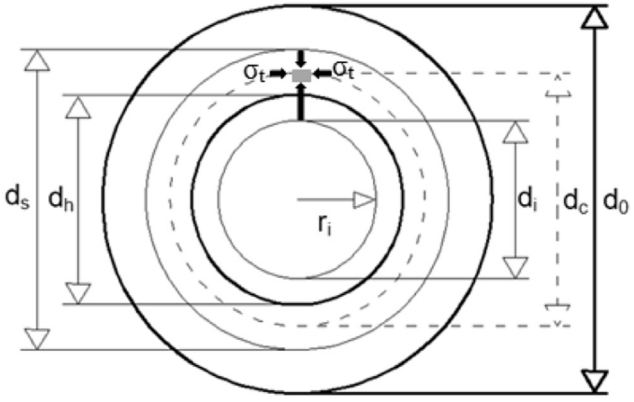

Fig. 5 – Scheme showing the diameters of envelope protector, polyethylene tube, and membrane where: σ_t = tangential tension d_o = the diameter for the external envelope protector; d_s = the inside envelope protector diameter and the outside membrane diameter; d_i = the inside membrane diameter; r_i = the inside membrane radius; d_h = the contact diameter; and, d_c = the equivalent membrane diameter after contraction.

Values for Δd_s and Δd_h, due to contact pressure (p_c), can be obtained either by applying Eq. (1) or Eq. (2). Therefore, B can be determined as:

$$B = \frac{p_C \cdot d_s}{E_s}\left(\frac{{d_s}^2 + {d_i}^2}{{d_s}^2 - {d_i}^2} - \nu_s\right) + \frac{p_C \cdot d_h}{E_h}\left(\frac{{d_0}^2 + {d_h}^2}{{d_0}^2 - {d_i}^2} + \nu_h\right) \quad (4)$$

By considering membrane contraction negligible in Eq. (4), d_s and d_h can be replaced by d_c without losing accuracy. Thus, the stress between the membrane and the tube (contact pressure p_c) could be calculated by:

$$p_C = \frac{B}{d_c\left[\frac{{d_c}^2 + {d_i}^2}{E_s\left({d_c}^2 - {d_i}^2\right)} + \frac{{d_0}^2 + {d_c}^2}{E_h\left({d_0}^2 - {d_c}^2\right)} - \frac{\nu_s}{E_s} + \frac{\nu_h}{E_h}\right]} \quad (5)$$

The value of p_C would correspond to the minimum operation pressure for the emitter and was estimated for a group of five randomly selected emitters. As p_C is reached, the emitter discharge will depend on the increase in the internal pressure which will change the diameter of the membrane according to Eq. (1).

There is a head loss through the water paths between the tube and the membrane that occurs under a gradually varied movement (membrane opening variation) after membrane compression. Besides, due to such loss, the membrane will have a smaller opening at the edge through which the water runs into the soil and thus, emitter obstruction can be avoided.

The Darcy–Weisbach general equation for pipe head losses (Eq. (6)) was used to estimate the membrane head loss, in which the membrane diameter deformation was calculated by considering its hydraulic radius (R_H) and Eq. (1).

$$H = \frac{f \cdot L \cdot q^2}{128 \cdot \pi^2 g \cdot {R_H}^5} \quad (6)$$

The head losses (H) along the membrane length (L) were estimated by adding the head losses from each length increment of 0.1 mm and by considering the friction factor (f), the hydraulic radius (R_H), the emitter discharge (q) and the gravity acceleration (g). By applying the energy equation between the emitter's centre and its end, it was possible to determine the energy available throughout the emitter.

The changes in the internal diameter (Δd_i) of the membrane, subjected to internal pressure (p_i) of 150 kPa, were estimated by laboratory tests that considered the Poisson coefficient (ν) of 0.5, the external diameter (d_s) and the elasticity module of the material (E) under 1000 kPa. The values for ν and E were obtained from the manufacturer of the emitter components although they could be determined by testing the material in the laboratory using appropriate tools.

The estimations of p_c by Eq. (5) and the experimental observations were compared by using the Pearson's correlation coefficient (r); and, their accuracy was quantified by Willmott's concordance index (d), (Willmott, 1982) following Eqs. (7) and (8). The coefficient "r" shows the dispersion between the measured point and its average value (random error), and the "d" index describes the relative co-variability between estimations and observations.

$$r = \frac{\left(n\sum_{i=1}^{n} E_i O_i\right) - \left(\sum_{i=1}^{n} E_i\right)\left(\sum_{i=1}^{n} O_i\right)}{\left\{\left[\left(n\sum_{i=1}^{n} (E_i)^2\right) - \left(\sum_{i=1}^{n} E_i\right)^2\right]\left[\left(n\sum_{i=1}^{n} (O_i)^2\right) - \left(\sum_{i=1}^{n} O_i\right)^2\right]\right\}^{0.5}} \quad (7)$$

$$d = 1 - \frac{\sum_{i=1}^{n} |E_i - O_i|}{\sum_{i=1}^{n} \left(|E_i - \overline{E}| + |O_i - \overline{O}|\right)} \quad (8)$$

where E_i and O_i are the estimated and observed data, respectively, n is the number of data, and $\overline{E}$ and $\overline{O}$ correspond to the average data.

The water application uniformity was calculated by applying the water emission uniformity coefficient CUE (Eq. (9)) proposed by Karmeli and Keller (1974) and was analysed according to ASABE Standards (1996). The manufacturer's coefficient of variation (CV_m) was calculated by Eq. (10). Both indices were determined on an emitter testing bench with a sample of 10 emitter units.

$$CUE = 100\left(1 - 1{,}27\frac{CV_m}{\sqrt{n}}\right)\frac{q_{min}}{q_m} \quad (9)$$

$$CV_m = 100\left(\frac{\sigma}{q_m}\right) \quad (10)$$

where q_{min} and q_m are the minimum and the average emitter discharges, respectively, n is the number of emitters and σ is the emitter discharge standard deviation.

2.3. *Experimental setup*

The performance of the designed emitter was determined in the laboratory and the experimental field station at the Biosystems Engineering Department of the University of São Paulo, SP – Brazil. An SDI system was installed within the protected environment of a greenhouse on July 7th, 2010. The emitters supplied water to two pot groups: one with bare soil (SS) and the other one with sugar cane (SC). The sugar cane variety was the RB867515 and was planted in clayey soil classified as Oxisol.

The irrigation design consisted of a 10 m long lateral line with 10 emitters spaced 1 m apart and buried at 20 cm, the depth at which the maximum concentration of the sugar cane roots is found. The emitters' location followed the horizontal direction coinciding with the sugar cane planting conditions in the field and other possibilities were not taken into consideration.

The pots were irrigated every 3 days during the first stage of sugar cane growth, and every 2 days during the following stages. The irrigation time varied according to the soil moisture content measured with a soil humidity sensor (automated tensiometer). On average, it took 20 min in the initial phase (6 months after planting), and 35 min from month 6 to month 18 (sugarcane harvesting), although the irrigation system was kept in the field for 12 months more. Therefore, the emitters operated for approximately 207 h and their performance was evaluated on October 7th, 2010 (three months after installation) and on January 7th, 2012. The visual

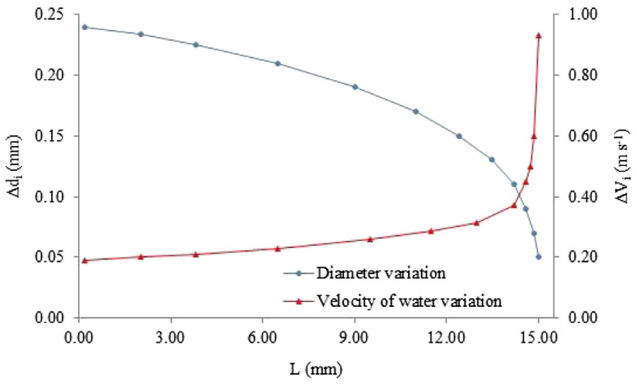

Fig. 6 – Changes in the membrane diameter (Δd_i) and velocity of water (Δv_i) along the length (L) of the membrane for the operating pressure $p = 150$ kPa.

inspection to look for obstruction by roots and soil particles was made at the end of the experiment.

The emitter's discharge was measured every three months after field installation using a flow-meter (magnetic inductive model IFC-090-F manufactured by Krohne) applying a full scale from 0 to 10 l h^{-1} with 99.97% accuracy. Such equipment was considered adequate for measuring the flow rate in the buried emitters. The operating pressure was controlled by an accurate digital manometer.

The emitters were inserted into a microtube, as shown in Fig. 2B, and then punched into the irrigation lateral line. The values of emitter flow rates were transferred to a data logger connected to both the microtube and the lateral line. It is noted that a steady electrical voltage is required to avoid pumping operation malfunctions which would change the operating pressure and, consequently, the emitter discharge. Attention should also be given to monitor water temperature variation, although it was not monitored in this study.

The measurements of emitter discharge were used to calculate the following indices: CUE (Eq. (9)); relative flow rate (QR) in the irrigation lateral line (Eq. (11)); disturbance of emitter flow (DQ) (Eq. (12)). These indices change according to the variations in the emitter flow and they will be affected, among other factors, by emitter clogging.

$$QR = \frac{Q_2}{Q_1} \tag{11}$$

$$DQ = 100\left(1 - \frac{Q_2}{Q_1}\right) \tag{12}$$

Likewise, the variation coefficient of relative flow (CV_{QR}), according to ASABE (2003), for the manufacturer's coefficient of variation was also determined as:

$$CVQR = \frac{\sigma_{QR}}{q_m} \tag{13}$$

where Q_1 and Q_2 are the average flow rate at the start and at the end of the field tests, and σ_{QR} is the standard deviation of the relative flow rate.

3. Results and discussion

3.1. Emitter prototype

For pressure $p = 150$ kPa, Δd_i decreased 4.5 times in moving from the membrane centre (point "0", 0.240 mm) to the edge of the membrane (0.053 mm). Likewise, Δv_i increased until reaching a value equivalent to the available pressure at the edge of the membrane (emitter discharge section), as shown in Fig. 6.

The variation in membrane's diameter calculated by Eq. (1) was used to estimate the value that corresponds to the emitter operation pressure. Furthermore, it can predict what the maximum membrane variation is for a given emitter flow rate by avoiding/diminishing root intrusion.

Considering the symmetry in the emitter's geometry (see Figs. 1–5), the pressure exerted by the water within the membrane must also be symmetric, so the tensions caused by external actions and the water pressure acting on the membrane will be independent of variable θ (see Fig. 4) though, for some emitters, it has been observed that water can discharge as a jet. This could be due to preferential flow through a possible channel developing between the membrane and the polyethylene tube, and this might be explained by a lack of physical homogeneity in the membrane material, although this should be assessed in further studies. Thus, the determination of the pressure for a given deformation of the membrane (variation of its radius r) can be accomplished if the pressure variation along the wall thickness is known (the only relevant variable is r). Likewise, as stated in Eq. (1), the change in r modifies the diameter of the membrane as pressure changes. Since pressure varies along the length of the membrane, the deformation (compression) of the membrane is also variable and, since it is made of an elastic material, the membrane deformation will be lower at the emitter outlet (considering constant flow and including head losses). The energy at this point will be, approximately, equal to the velocity of the water squared divided by twice the acceleration of gravity.

In addition, the relation between the Darcy–Weisbach head loss equation and the membrane's diameter variation can be used to estimate the emitter's flow rate variation, between the membrane opening and the tube from the hole to the water exit, for a given operation pressure. The elastic membrane plays a flow rate regulator role in this study, a fact that can also minimise intrusion by roots and soil particles into the emitter.

Table 1 shows the estimated minimum operating pressure p_c for five emitters, and their physical features. Values of p_c changed with the variation of $|d_h - d_s|$ and $|d_h - d_i|$ and this variation is justified by the differences in the emitters' physical features. Pressure variation within each emitter was mainly affected by the inner and outer diameters of the membrane, by the inner diameter of the protector system and by the outer diameter of the polyethylene tube. The variation in the outer diameter of the envelope protector and in the inner diameter of the polyethylene tube did not have a significant effect upon p_c. This could be explained by the fact that the elasticity modulus of both the envelope protector and the

Table 1 – Minimum operating pressure and physical characteristics of some emitters.

Emitter	1	2	3	4	5
Minimum operation pressure – p_c (kPa)					
p_c	115	98	100	105	110
Physical characteristics dimensions (mm)					
L_m	30	31	31	31	30
d_{im}	6.9	7.0	7.0	6.8	6.9
d_s	13.5	13.1	13.3	13.2	13.3
d_{it}	5.5	5.7	5.7	5.7	5.9
d_h	7.5	7.4	7.5	7.3	7.4
d_{sp}	12.4	12.4	12.5	12.4	12.5
d_o	30.0	30.0	30.0	30.0	30.0
$\lvert d_h - d_i \rvert$	0.6	0.4	0.5	0.5	0.5
$\lvert d_h - d_s \rvert$	6.0	5.7	5.8	5.9	5.9

Note: d_o = the diameter for the outside envelope protector; d_s = the inside envelope protector diameter; d_i = the inside membrane diameter; r_i = the inside membrane radius; d_s = the outside pipe diameter; d_h = the contact diameter; and d_c = the equivalent membrane diameter after contraction.

polyethylene tube were much greater than that of the membrane. The highest p_c value was coincident with the highest $|d_h - d_i|$ value, which is beneficial to avoid root intrusion inside the emitter, otherwise more energy would be needed to achieve the highest pressure.

The emitter operating pressure calculated by Eq. (5) could be used for selecting the best material to use for the membrane and it could reduce production cost and time throughout the development of the emitter prototype. However, it is necessary to consider the material's physical features such as: dimension, elastic modulus and Poisson coefficient.

The observed pressures and their estimated values using Eq. (6) showed good agreement (Fig. 7) with a Pearson correlation coefficient $r = 0.9$, similar to that found in a study by Santos (2007), and a Willmott concordance index = 0.85. Thus, it is likely that the elasticity module and Poisson coefficient selected for characterisation of membrane material were correct. These variables could not be determined in the laboratory due to lack of equipment, but this is recommended in further research.

As mentioned in Section 2.1, due to lack of specific equipment for handcrafting the emitter, this was made of a silicone membrane, a PVC protector and a polyethylene tube. These materials are available in the market and they fulfil the minimum requirements for handmade products and the basic functioning principles applied to them (mechanical-hydraulic mechanism to open and close the emitter). However, the chosen materials might be modified and enhanced. Also, the size of the emitter could be modified and its behaviour could be extrapolated by using dimensional and similarity analysis. Although a cylindrical membrane was studied, other geometries, such as a rectangular membrane, could also be tested in further studies.

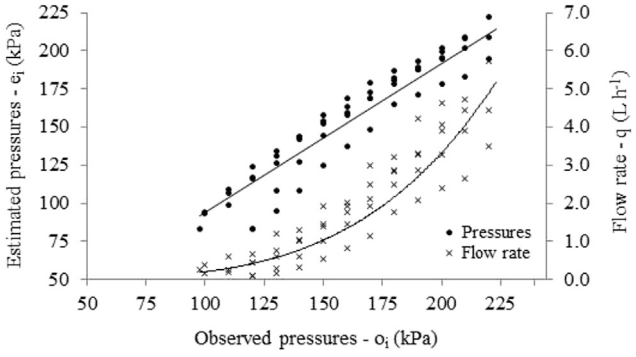

Fig. 7 – Relation between estimated (e_i) and observed (o_i) pressures, and observed emitter's flow rate.

3.2. *Assessment of the emitters' performance*

The spatial and temporal flow rate variation in the emitter was negligible in both soils (SC and SS) from July 2010 to January 2012. They presented median values ranging from 1.2 to 2.2 l h^{-1} (see Fig. 8). Unfortunately, obstruction could not be the cause since the flow variation occurred within all emitters, at the same time. It might be explained by changes in the soil back pressure which could have changed the flow rate. In fine textured soils, as used in this study, the emitter flow rate can exceed soil infiltration so that water accumulates around the emitter outlet until both stabilise, and there is therefore an overpressure ("back pressure")in the soil surrounding the emitter. Such pressure would reduce the emitter discharge (Gil, Rodriguez-Sinobas, Juana, Sánchez, & Losada, 2008). Also, since temperature was not monitored and the emitter discharge exponent was higher than 0.5, temperature variation could also have changed the emitter discharge (Rodriguez-Sinobas,Juana, & Losada, 1999). Thus, monitoring water temperature during the field tests should be addressed in further research. In addition, it would be interesting to develop a pressure compensating element to reduce the soil backpressure effect on the emitter discharge.

In general, the SS and SC tests followed a similar pattern by decreasing and increasing the emitter flow rate during field evaluation. An exception to such behaviour was observed for the SS in which the emitter flow rate decreased in the last two

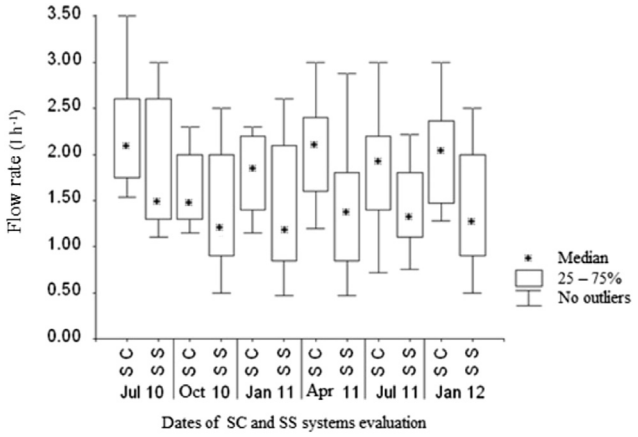

Fig. 8 – Emitters' flow rate during the field evaluation (Note: SC = pots containing sugar cane, and SS = pots containing bare soil).

Table 2 – Relative flow (QR), water emission uniformity coefficient (CUE), manufacturer's coefficient of variation (CV_m) and variation coefficient of relative flow rate (CVQR).

Period of evaluation	System		Period of evaluation	System	
	SC	SS		SC	SS
	$QR_{média}$ (dimensionless)			CV_{QR} (%)	
Oct 2010	0.75 Ba	0.74 Ba	Oct 2010	25.70	25.90
Jan 2011	0.81 Ba	0.85 Ba	Jan 2011	13.75	26.38
Apr 2011	0.92 Aa	0.81 Ba	Apr 2011	12.83	24.30
Jul 2011	0.81 Ba	0.81 Ba	Jul 2011	19.50	25.10
Jan 2012	0.89 Aa	0.84 Ba	Jan 2012	12.26	23.82
Average	0.84 b	0.81 b	Average	16.21	25.10
Period of evaluation	System		Hydraulic evaluation	System	
	SC	SS		SC	SS
	CUE (%)				
Out 2010	58.00	52.29	CUE (%)[a]	58.70	59.85
Jan 2011	57.60	52.10	CV_m (%)[a]	37.98	40.00
Apr 2011	50.00	50.00			
Jul 2011	54.60	46.57			
Jan 2012	55.45	48.23			
Average	53.33	49.84			

Means followed by the same letter, lowercase and uppercase in the column and in the line, respectively, do not differ by Tukey test at 1%.
SC – System with sugar cane crop.
SS – System with bare soil.
[a] Initial evaluation.

evaluations, thus indicating that the change was not caused by root intrusion.

Table 2 shows the coefficients calculated by applying Eqs. (9)–(13) for all the evaluations. CUE was classified as nonstandard according to ASABE (1996) for both groups (SC and SS). Water application uniformity hardly changed over time. However it was low and requires further improvement. The CUE and CV_m indexes were low for the SC and high for the SS. This indicates a poor manufacturing process since the emitter units were handcrafted in a lathe. Likewise, variations over time in QR and CV_{QR} might be caused by factors such as water temperature variations and soil back pressure. However the mean QR values for SC and SS were statistically identical.

Table 3 shows the disturbance in the emitter flow (DQ) and it matches the field evaluations from October, 2010 to January, 2012. These evaluations present a similar trend to that for CV_{QR} (see Table 2). It is noteworthy that although DQ values ranged between 16% and 24%, the CV_{QR} values were high and similar to the CUE values (Table 1). However, these values did not show any clear trend. The mean DQ value for the SS pots was higher than that for the SC pots, and it clearly shows that this difference depends on the culture and the soil only.

Table 3 – Disturbance of emitter's flow rate (DQ) during the field evaluations from October, 2010 to January, 2012 using two pot groups: bare soil (SS) and the other one with sugar cane (SC).

Dates of evaluations	SS system	SC system
	DQ (%)	
Oct 2010	20.0	24.0
Jan 2011	20.0	23.4
Apr 2011	18.0	18.5
Jul 2011	18.0	23.0
Jan 2012	16.0	23.5
Average	18.3	22.5

Emitter clogging caused by suction of soil particles or root intrusion was not observed during the field tests, thus corroborating the high and low values shown for CV_{QR} and CUE, respectively. The lower QR values (see Table 2) did not correspond to clogging, as earlier described in the text, but they may relate to physical limitations of the silicone material used for the membrane. The combined effect of compression and tension on the walls might have affected the membrane's elasticity and the flow rate within the emitter during the field tests.

It is worth noting that the basic goal of the current study was the design, hand manufacture and evaluation of an emitter prototype that could avoid soil and root intrusion without the application of chemicals. The design evaluated in this study is simple but has shown potential to prevent root intrusion. Moreover, the novel approach fostered by the present study could be a tool to pursue such goal. This is the first emitter prototype to be evaluated but further development is still needed to address the issues mentioned above (such as the search for the best material for the emitter's membrane in order to regulate emitter discharge) before considering commercially manufacture. Nevertheless, the methodology presented in this work could save time and could reduce the cost during the manufacturing process if it is applied to improve the actual emitter design or similar emitter geometries.

4. Conclusion

One of the drawbacks presented by SDI is emitter obstruction caused by soil particles and root intrusion. Nowadays, there is a concern about the use of chemicals to avoid this problem. The novel emitter geometry developed for SDI whose operation has been explained by hydraulic and mechanical principles, adequately prevented the entry of roots and soil particles in the emitter throughout the evaluation period.

The approach proposed, which considers the general Darcy–Weisbach head loss equation and the diameter variation of the elastic membrane, may be a useful tool for future studies on the adaptation of the present emitter prototype to the commercial phase or on similar emitter geometries and similar hydraulic-mechanical operation. This could consider other materials than the ones in this study. Furthermore, it could also be used to estimate the emitter minimum operation pressure, to determine variations in the diameter of the emitter membrane, and to estimate the emitter discharge due to changes in the membrane's diameter. Its application in emitter design could save time and reduce the cost of manufacture.

Acknowledgements

The authors would like to thank: the University of São Paulo, Department of Biosystems Engineering and Sao Paulo State Research Foundation for funding this study; the personnel of the "Hydraulic for Irrigation" research group (Technical University of Madrid) for their valuable contribution for the analysis on the emitter prototype. Finally, the Spanish Ministry of Science and Technology (CICYT) for its support provided through project N. AGL2008-00153/AGR.

REFERENCES

Abdulqader, A., & Mohammed, A. (2013). Anti-clogging drip irrigation emitter design innovation. *European International Journal of Science and Technology, 08*, 154–164.

ASABE Standards. (1996). *Field evaluation of microirrigation systems*. ASAE EP 458.

ASABE Standards. (2003). *Design and installation of microirrigation systems*. ASAE EP405.1.

California University. (2008). *Maintaining irrigation system*. Publication 21637. Agricultural and Natural Resources.

Cloi, C. Y., & Suarez-Rey, E. M. (2004). Subsurface drip irrigation for bermudagrass with reclaimed water. *American Society of Agricultural Engineers, 47*, 1943–1951.

Coelho, R. D., Faria, L. F., & Mélo, R. F. (2006). Variação de vazão em gotejadores convencionais enterrados por intrusão radicular na irrigação de citros. *Irriga, 11*, 230–245.

Dasberg, S., & Or, D. (1999). *Drip irrigation*. Berlin, Germany: Springer-Verlag.

Gil, M., Rodriguez-Sinobas, L., Juana, L., Sánchez, R., & Losada, A. (2008). Emitter discharge variability of subsurface drip irrigation in uniform soils: effect on water-application uniformity. *Irrigation Science, 26*, 451–458.

Hearn, E. J. (1997). *Mechanics of materials 1: An introduction to the mechanics of elastic and plastic deformation of solids and structural components* (3rd ed.). Oxford, New York: Butterworth Heinemann.

Hernandez, M. G. (2010). Proteção de gotejadores à obstrução por intrusão radicular em irrigação subsuperficial de figueiras. In *Programa de Pós-Graduação em Engenharia Agrícola*. Santa Maria, RS: Universidade Federal de Santa Maria – RS.

Karmeli, D., & Keller, J. (1974). Trickle irrigation design parameters. *Transactions of the ASAE, 17*, 678–684. St. Joseph, Mich.

Mosca, M. A., Testezlaf, R., & Gomes, E. E. (2005). Desenvolvimento de emissores alternativos para irrigação subsuperficial de baixa pressão. *Irriga, 10*, 249–262.

Rodríguez-Sinobas, L., Gil, M., Sánchez, R., & Benitez, J. (February 2012). Simulation of soil wetting patterns in drip and subsurface drip irrigation. Effects in design and irrigation management variables. *Soil Science (Wolters-Kluwer), 177*(2), 1–6. http://dx.doi.org/10.1097/SS.0b013e3182411317.

Rodriguez-Sinobas, L., Juana, L., & Losada, A. (1999). Effects of temperature changes on emitter discharge. *Journal of Irrigation and Drainage Engineering, 125*, 64–73.

Santos, C. (2007). *Estatística descritiva: Manual de auto-aprendizagem*. Lisboa: EdiçõesSilabo.

Souza, W. De. J. (2012). Protótipos e avaliação de emissores para irrigação localizada subsuperficial. In *Programa de Pós-Graduação em Engenharia de Biossistemas*. Piracicaba, SP: Universidade de São Paulo–SP.

Suarez-Rey, E. M., Choi, C. Y., McCloskey, W. B., & Kopec, D. M. (2006). Effects of chemicals on root intrusion into subsurface drip emitters. *Irrigation and Drainage, 55*, 501–509.

Willmott, C. J. (1982). Some comments on the evaluation of model performance. *Bulletin of the American Meteorological Society, 63*, 1.309–1.313. Boston.